Electronic Supplementary Material (ESI) for Materials Chemistry Frontiers.

Supplementary Material for

Self-healable hybrids fabricated by metal complexation with imidazole-containing silsesquioxane nanoparticles

Yusuke Sasaki†, and Hideharu Mori*†

†Department of Organic Materials Science, Graduate School of Organic Materials Science, Yamagata University, 4-3-16, Jonan, Yonezawa, 992-8510, Japan

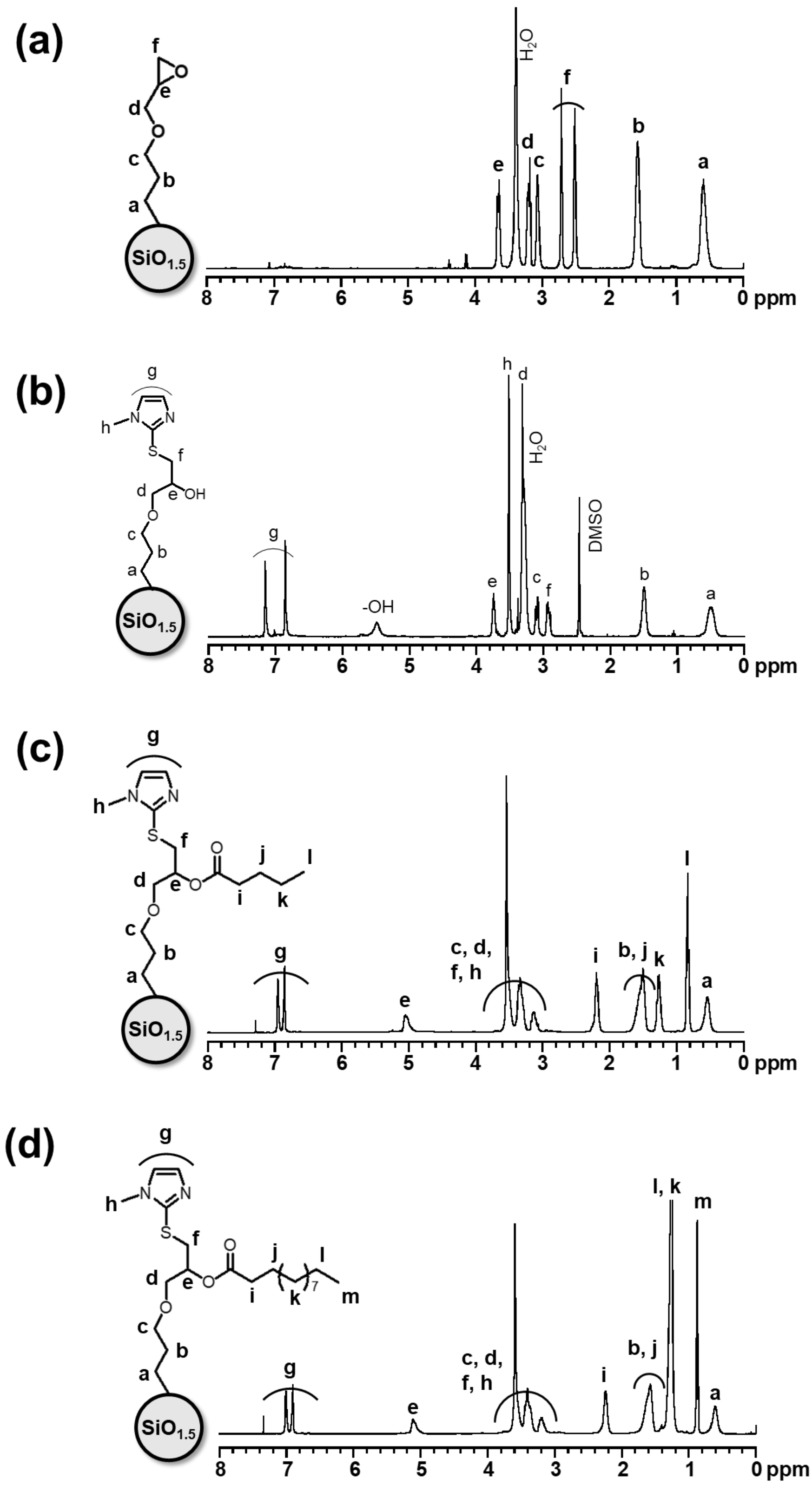

Figure S1. ^{1}H NMR spectra of (a) (Gly-$SiO_{1.5}$)$_n$, (b) (MI/OH-$SiO_{1.5}$)$_n$ (DMSO-d_6), (c) (MI/Bu-$SiO_{1.5}$)$_n$ and (d) (MI/Ud-$SiO_{1.5}$)$_n$ ($CDCl_3$)

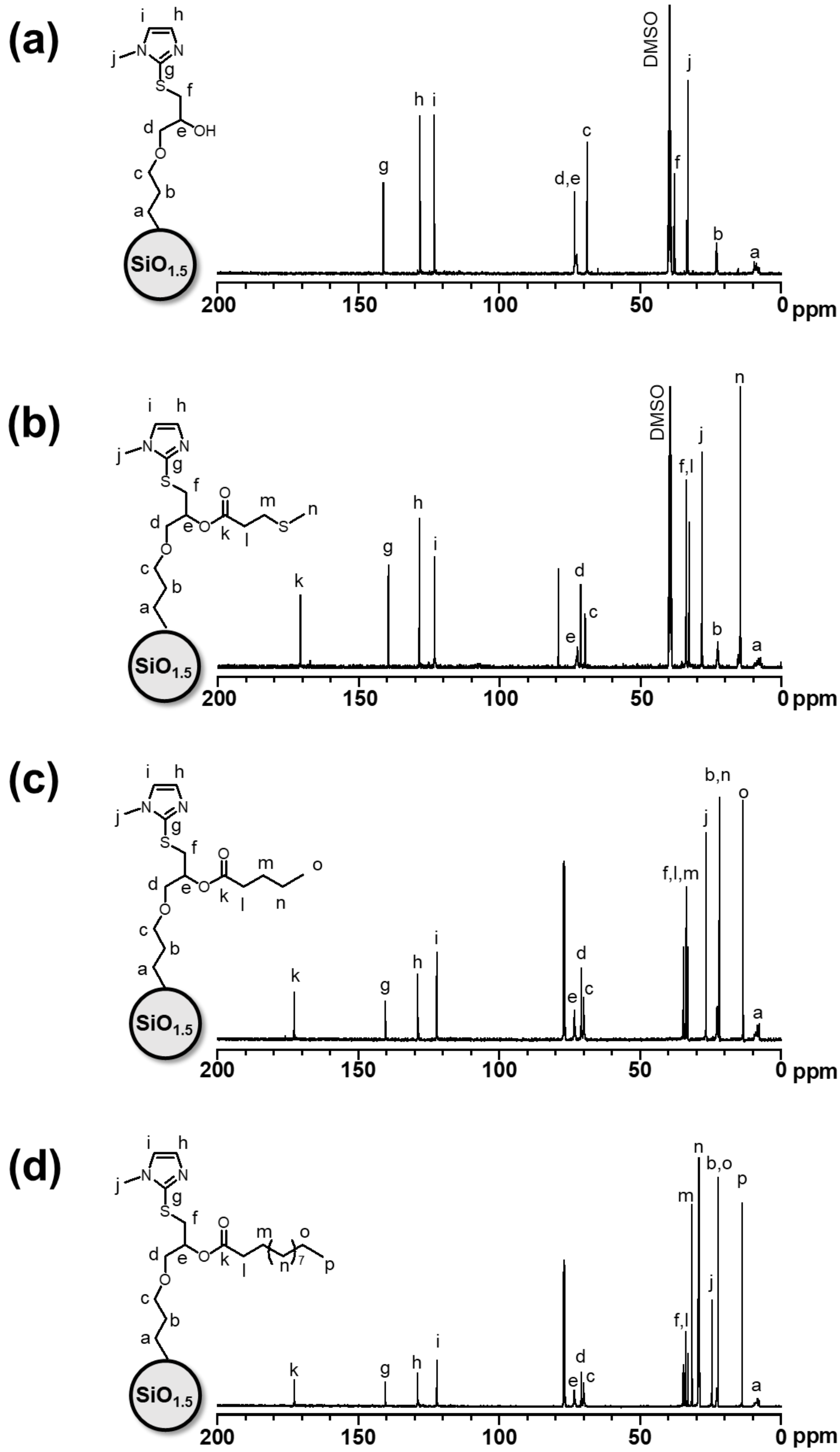

Figure S2. ^{13}C NMR spectra of (a) $(MI/OH\text{-}SiO_{1.5})_n$ (b) $(MI/MT\text{-}SiO_{1.5})_n$ (DMSO-d_6), (c) $(MI/Bu\text{-}SiO_{1.5})_n$ and (d) $(MI/Ud\text{-}SiO_{1.5})_n$ ($CDCl_3$)

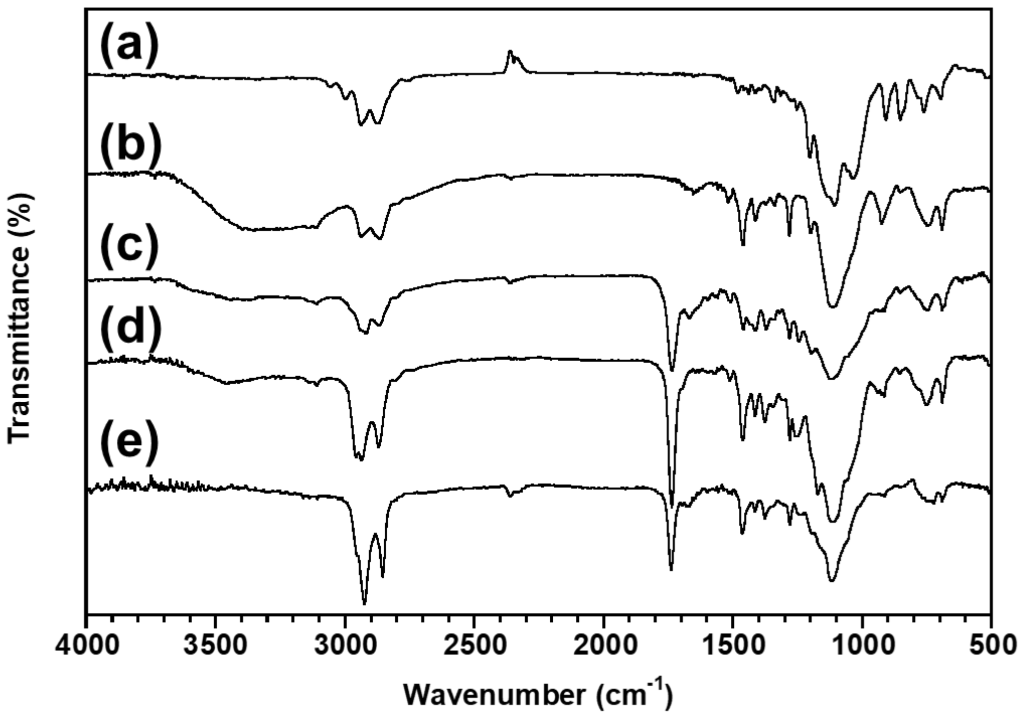

Figure S3. FT-IR spectra of (a) $(Gly\text{-}SiO_{1.5})_n$, (b) $(MI/OH\text{-}SiO_{1.5})_n$, (c) $(MI/MT\text{-}SiO_{1.5})_n$, (d) $(MI/Bu\text{-}SiO_{1.5})_n$, and (e) $(MI/Ud\text{-}SiO_{1.5})_n$.

Table S1. Solubility of SQ-NPs.

Entry	H_2O	MeOH	DMSO	DMF	Ace	THF	$CHCl_3$	Et_2O	Hex
$(Gly\text{-}SiO_{1.5})_n$ a)	−	−	+	−	−	−	−	−	−
$(MI/OH\text{-}SiO_{1.5})_n$	−	−	+	+	−	+	+	−	−
$(MI/MT\text{-}SiO_{1.5})_n$	−	−	+	+	−	+	+	−	−
$(MI/Bu\text{-}SiO_{1.5})_n$	−	−	+	+	−	+	+	−	−
$(MI/Ud\text{-}SiO_{1.5})_n$	−	−	−	−	−	+	+	−	−

+ = soluble at r.t. (1 mg/ml), − = insoluble at r.t., time = 1 day, a) time = 1 week.

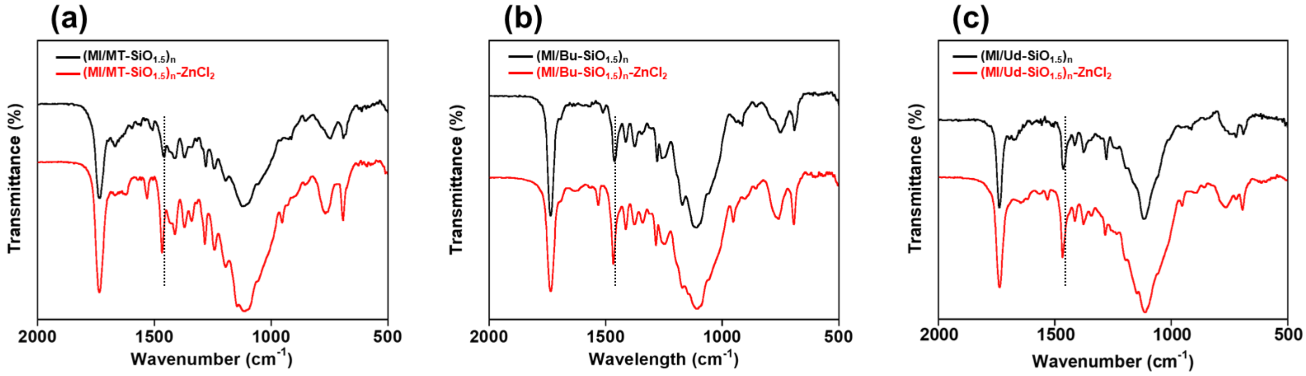

Figure S4. FT-IR spectra of (a) $(MI/MT\text{-}SiO_{1.5})_n\text{-}ZnCl_2$, (b) $(MI/Bu\text{-}SiO_{1.5})_n\text{-}ZnCl_2$, and (c) $(MI/Ud\text{-}SiO_{1.5})_n\text{-}ZnCl_2$ before and after metal complexation, respectively.

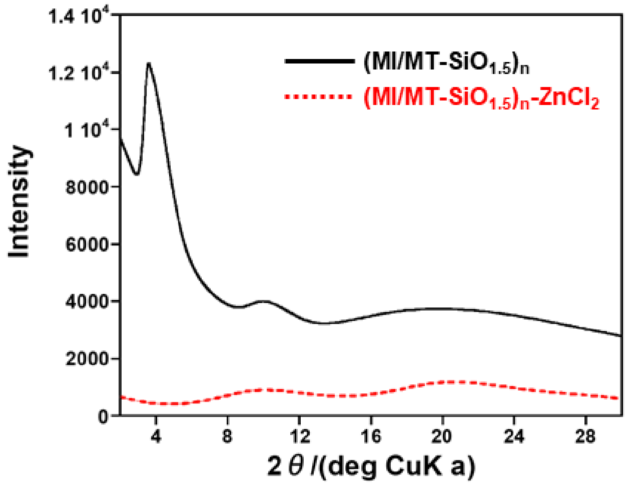

Figure S5. XRD profiles of $(MI/MT\text{-}SiO_{1.5})_n\text{-}ZnCl_2$ before and after metal complexation.

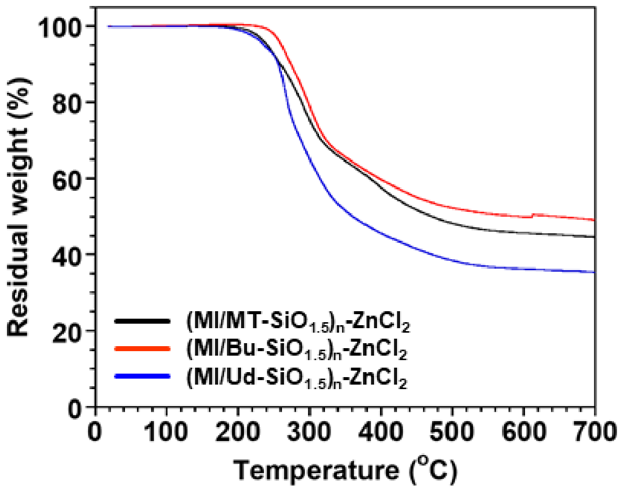

Figure S6. TGA thermograms of the imidazole-containing dual functional silsesquioxane nanoparticles (SQ-NPs) after metal complexation with $ZnCl_2$.

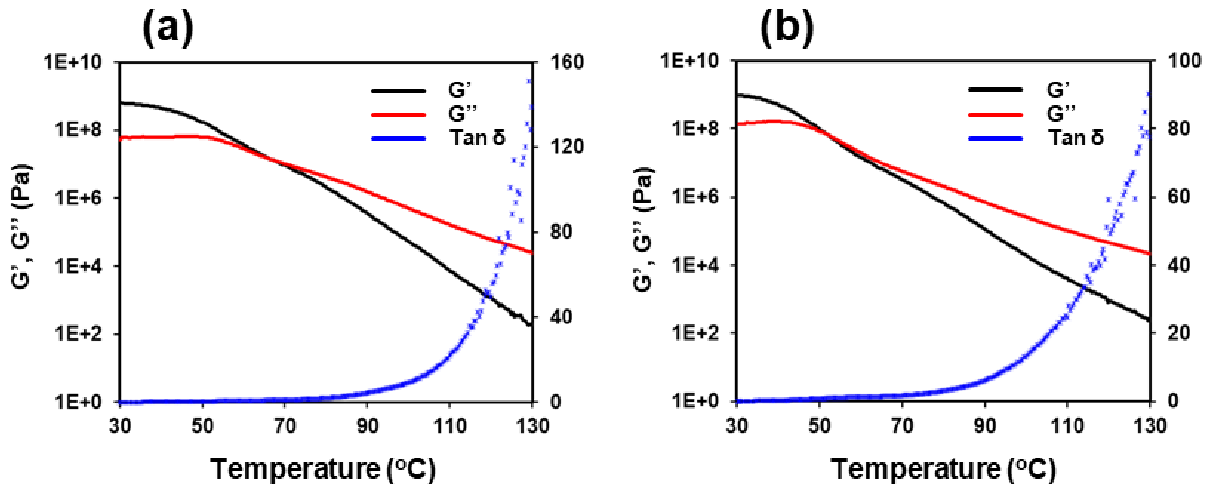

Figure S7. G', G″, and tan δ (G″/G') values of (a) $(MI/Bu\text{-}SiO_{1.5})_n\text{-}ZnCl_2$ and (b) $(MI/Ud\text{-}SiO_{1.5})_n\text{-}ZnCl_2$ recorded during the temperature dispersion tests in a range from 30 °C to 130 °C (2 °C/min) at a constant frequency of 1Hz at an applied strain (γ) of 0.01 to 0.1%.

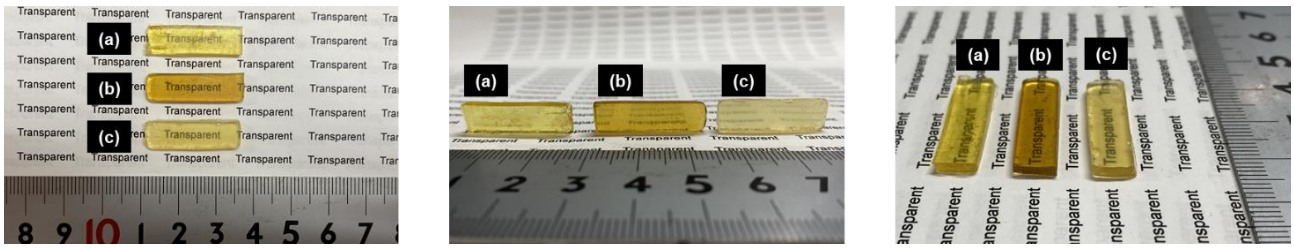

Figure S8. Fabricated rectangular (length; 25 mm, width; 7 mm, height; 2 mm) films; (a) $(MI/MT\text{-}SiO_{1.5})_n\text{-}ZnCl_2$, (b) $(MI/Bu\text{-}SiO_{1.5})_n\text{-}ZnCl_2$, and (c) $(MI/Ud\text{-}SiO_{1.5})_n\text{-}ZnCl_2$ for flexural stress-strain test.

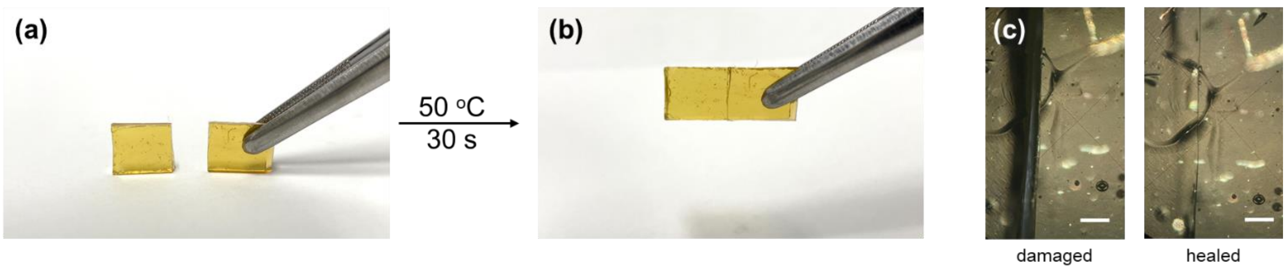

Figure S9. Preliminary self-healing test for $(MI/Bu\text{-}SiO_{1.5})_n\text{-}ZnCl_2$; (a) cut specimen into two pieces, (b) healed specimen after 30 s of contacting the damaged surface at 50 °C, (c) microscopic images of a film before (left) and after (right) healing at 50 °C. Scale bar 500 μm.

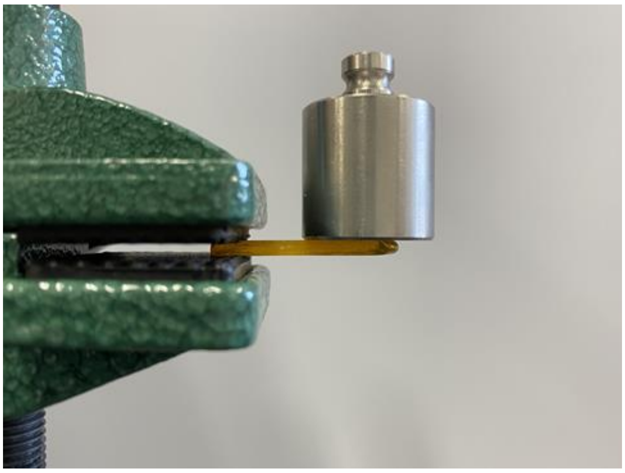

Figure S10. The healed specimen at 50 °C for 24 h, $(MI/Bu\text{-}SiO_{1.5})_n\text{-}ZnCl_2$, sustained the load of a 50 g.

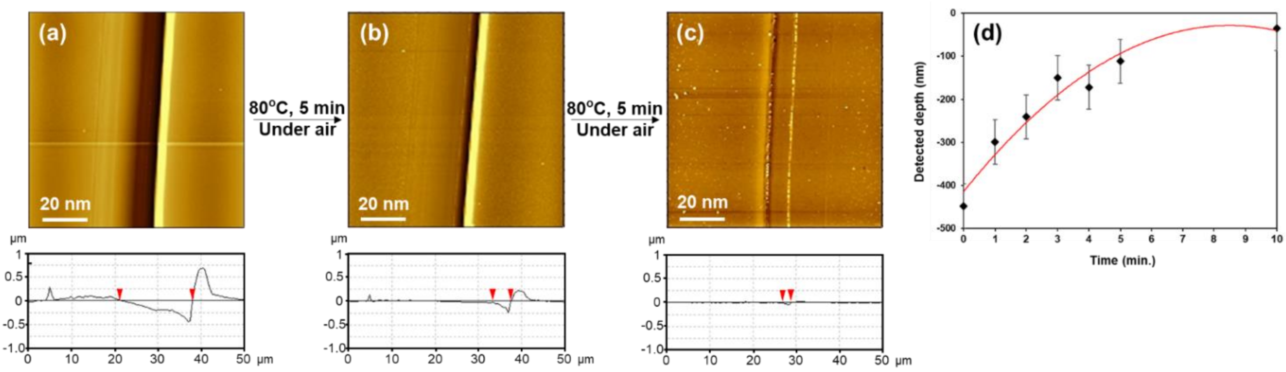

Figure S11. Time-dependent change in SFM height images (z-range = 1.30 μm) of the $(MI/MT\text{-}SiO_{1.5})_n\text{-}ZnCl_2$ hybrid film in the vicinity of the scratch. The sample was heated at 80 °C for (a) 0 min, (b) 5 min, and (c) 10 min.

Table S2. The mechanical properties of zinc/imidazole-based hybrids.

Entry	ε max (%)[a]	σ max (MPa)[b]	Young's modulus (GPa)[c]
$(MI/MT\text{-}SiO_{1.5})_n\text{-}ZnCl_2$	0.445 ±0.22	8.55 ±1.46	2.13 ±0.59
$(MI/Bu\text{-}SiO_{1.5})_n\text{-}ZnCl_2$	0.402 ±0.11	7.378 ±1.70	1.05 ±0.07
$(MI/Ud\text{-}SiO_{1.5})_n\text{-}ZnCl_2$	0.560 ±0.04	3.57 ±0.51	0.56 ±0.16

a) Ultimate extensibility, b) ultimate tensile stress, c) calculated from small strain region (0.05-0.25 %. The results were obtained from the flexural stress-strain tests.